

Linker editing of pneumococcal lysin ClyJ conveys improved bactericidal activity

Hang Yang^{1,2,*}, Dehua Luo³, Irina Etobayeva^{2,4}, Xiaohong Li¹, Yujing Gong³, Shujuan Wang¹,
Qiong Li⁵, Poshi Xu⁶, Wen Yin³, Jin He³, Daniel C. Nelson^{2,4,*}, Hongping Wei^{1,*}

Supporting information

Table S1. Secondary structure of ClyJ variants in the presence/absence of 50 mM choline.

Secondary Structure	Percentage of composition (%) ^a			
	ClyJ	ClyJ-1	ClyJ-2	ClyJ-3
Helix	17.0 (15.9)	17.3 (16.4)	16.8 (15.9)	16.8 (15.7)
Antiparallel	27.3 (29.4)	26.9 (28.8)	28.6 (30.5)	28.2 (30.6)
Parallel	14.3 (15.1)	14.0 (14.6)	14.2 (14.8)	14.3 (15.1)
Beta-Turn	20.9 (21.3)	20.9 (21.2)	21.1 (21.5)	21.1 (21.5)
Rndm. Coil	43.1 (44.5)	42.2 (43.3)	41.9 (43.0)	42.3 (43.9)

^aData shown in parentheses is generated in the presence of 50 mM choline.

Table S2. Transition temperatures of ClyJ variants in the presence/absence of 50 mM choline.

Variant	Transition temperature (°C)	
	without choline	with choline
ClyJ	41.8	40.1/56.6
ClyJ-1	42.3	40.7/57.0
ClyJ-2	43.1/51.5	42.4/59.9
ClyJ-3	43.8	44.5/57.1

Table S3. Bacterial strains used in this study.

	Strains	Characteristic	Source
<i>Pneumococci</i>	NS26		a
	NS20		a
	Lyt 4.4	Derived from R6, LytA non-functional	b
	R6	Derived from R36A	b
	DCC1490	Serotype 14	b
	DCC1420	Serotype 23F, clonal type Sp23-1	b
	DCC1850	Serotype 6	b
	DCC1335	Serotype 9V, clonal type Sp9-3	b
	765		b
	R36A	Derived from D39, capsule free strain	b
	D39	Serotype 2	b
	DCC1811	Serotype 11	b
	763		b
	#8		b
	DCC1494	Serotype 14, clonal type Sp14-3	b
	DCC1714	Serotype 3	b
	AR620	Serotype 1	b
	TIGR4		b
	GB2163	Serotype 10	b
	GB2092	Serotype 4	b
Non-pneumococci	<i>S. mutans</i> ATCC 25175		b
	<i>S. gordonii</i> PK488		b
	<i>S. rattus</i> BHT		b
	<i>S. salivarius</i> ATCC 27945		b
	<i>S. parasanguis</i> PK2564		b
	<i>S. intermedius</i> PK2821		b

<i>E. coli</i>	<i>E. coli</i> BL21(DE3)	Protein expression host	a
	BL21-pET- <i>cpl-1</i>	BL21(DE3) with pET28b- <i>cpl-1</i>	a
	BL21-pET- <i>clyJ</i>	BL21(DE3) with pET28b- <i>clyJ</i>	a
	BL21-pET- <i>clyJ-1</i>	BL21(DE3) with pET28b- <i>clyJ-1</i>	c
	BL21-pET- <i>clyJ-2</i>	BL21(DE3) with pET28b- <i>clyJ-2</i>	c
	BL21-pET- <i>clyJ-3</i>	BL21(DE3) with pET28b- <i>clyJ-3</i>	c

a. Lab collection at Wuhan Institute of Virology, Chinese Academy of Sciences, Wuhan, China. **b.** Lab collection at Institute of Biotechnology and Biological Sciences, University of Maryland, Rockville, Maryland, USA. **c.** This work.

Table S4. Primers used in this study.

Primer	Sequence (5'-3')	Restriction site
ClyJ-1-F1	tataccatgggcatggcagcaaatctgg	<i>NcoI</i>
ClyJ-1-R1	tataggatccggaggatcctcctttgaaggtaac	<i>BamHI</i>
ClyJ-1-F2	tataggatccggtgatccgtatccgtatctg	<i>BamHI</i>
ClyJ-1-R2	tatactcgagtttggtggaatcagaccgtcc	<i>XhoI</i>
ClyJ-2-F1	tataccatgggcatggcagcaaatctggcaaacgcacaagcaca	<i>NcoI</i>
ClyJ-2-R1	tataggatccggaggatcctccggatccggaggatcctcc	<i>BamHI</i>
ClyJ-3-R1	cccagggatccggaggatcctccttt	
ClyJ-3-F2	aaaggaggatcctccggatccctgg	

Figure S1. Analysis of the CBDs from ClyJ, Cpl-1, and LytA. Aligned sequences were analyzed by ESPript 3.0 online software (<http://esprict.ibcp.fr/ESPript/cgi-bin/ESPript.cgi>) using the crystal structure of LytA (pdb: 4X36) as a template. Strict α - and β -turns are rendered as TTT and TT. Six choline binding repeats (CBR1-6) and the C-terminal tail (C-tail) are indicated.

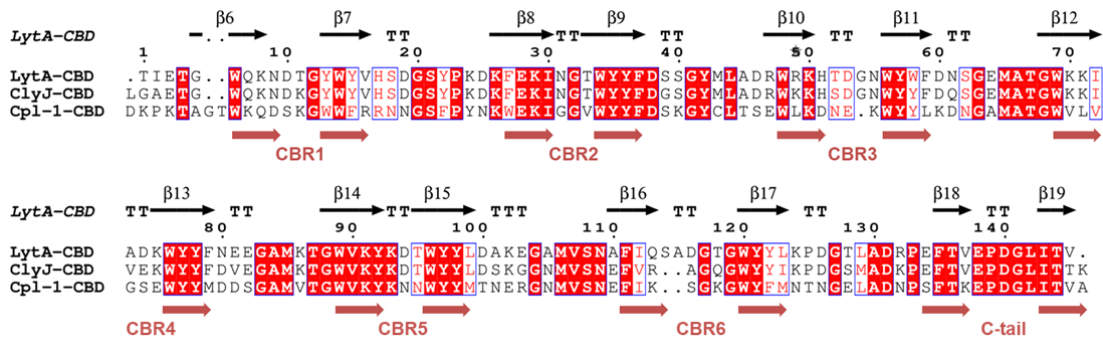


Figure S2. Analysis of the linker sequences of ClyJ and its variants. Aligned sequences were analyzed by ESPript 3.0 online software (<http://esprict.ibcp.fr/ESPript/cgi-bin/ESPript.cgi>).

	1		10		20
ClyJ-linker	GS	VDPYPYLAKWGSREQFKRDIENG	
ClyJ-1-linker	GGSS	GS	VDPYPYLAKWGSREQFKRDIENG	
ClyJ-2-linker	GGSS	GS	GGSSGS	VDPYPYLAKWGSREQFKRDIENG	
ClyJ-3-linker	GGSS	GS	

Figure S3. SDS-PAGE analysis of ClyJ and its variants. Enzymes were purified from *E. coli*, dialyzed against PBS, and analyzed by 12% SDS-PAGE. M: standard protein markers.

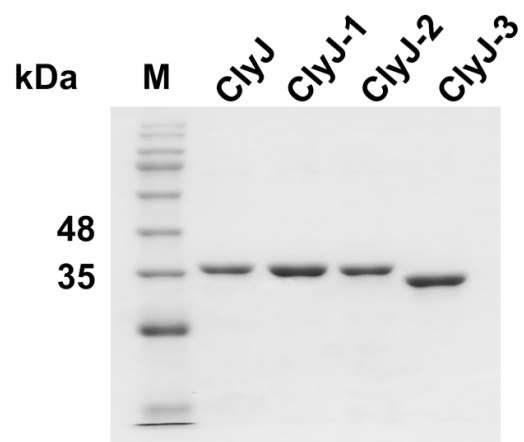


Figure S4. Structural predictions for ClyJ and its variants. Protein sequences were analyzed by the I-TASSER online service (<https://zhanglab.cmb.med.umich.edu/I-TASSER/>). Structures with the highest confidence are presented. The EAD is colored in green, the binding domain is red, and linker region is cyan. Based on the predicted model, the confidence score (C-score), estimated template modeling score (TM-score), and estimated root mean square deviation (RMSD) for the ClyJ model are -2.00, 0.48 ± 0.15 , and $11.0\pm 4.6\text{\AA}$, respectively. The C-score, estimated TM-score, and estimated RMSD for the ClyJ-1 model are -0.51, 0.65 ± 0.13 , and $7.5\pm 4.3\text{\AA}$, respectively. The C-score, estimated TM-score, and estimated RMSD for the ClyJ-2 model are -2.61, 0.41 ± 0.14 , and $12.6\pm 4.3\text{\AA}$, respectively. The C-score, estimated TM-score, and estimated RMSD for ClyJ-2 model are -1.80, 0.50 ± 0.15 , and $10.4\pm 4.6\text{\AA}$, respectively. The C-score is calculated based on the significance of threading template alignments and the convergence parameters of the structure assembly simulations. TM-score and RMSD are known standards for measuring structural similarity between two structures.

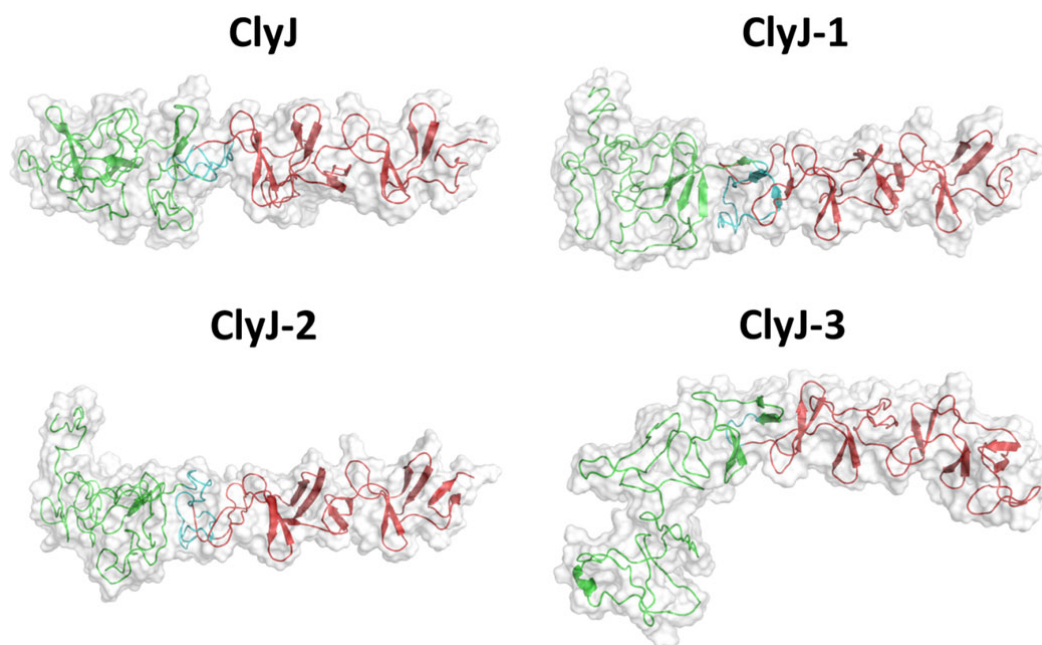


Figure S5. Polymerization analysis of ClyJ. ClyJ was crosslinked with 1.5 mM BS(PEG)₉ in the absence or presence of 50 mM choline at room temperature for 30 min, and analyzed by 12% SDS-PAGE.

